Human Biological Clock and Planetary Temperature Distribution Determined by Relativistic Matter Wave

Huaiyang Cui
Department of Physics, Beihang University, Beijing, 102206, China
Email: hycui@buaa.edu.cn
(March 15, 2023, submitted to viXra)

Abstract: Relativistic matter wave provides a biological clock for human beings, it also governs planetary size and temperature. In this paper, the sunspot period, earth's atmosphere circulation with season clock and human biological clock are investigated, the clock formula is derived. As the results, the period of sunspot cycle is calculated to be 10.93 years, the human mean lifespan on the Earth is calculated to be 84 years, while the human mean lifespan reduces to 8.6 years on the Mars. A guidance of anti-ageing is proposed for the biological clock. The solar radius is determined as 7e+8 (m) with a relative error of 0.72%; the earth's radius is determined as 6.4328e+6 (m) with a relative error of 0.86%. The temperatures in the solar interior and in the earth's interior are also calculated by their relativistic matter waves. This approach gives a temperature 6031K in the solar convective layer, the solar core shell is estimated at a temperature 852K. The atmospheric temperature at sea level in the equatorial region is estimated to be 293K, and the mantle temperature is estimated to be 1467K.

Key words: relativistic matter wave, biological clock, temperature distribution.

1. Introduction

This year is 100th anniversary of the initiative of de Broglie matter wave. In 1923, the Louis de Broglie considered blackbody radiation as a gas of light quanta [1], he tried to reconcile the concept of light quanta with the phenomena of interference and diffraction. In 1923 and 1924, the concept that matter behaves like a wave was proposed by Louis de Broglie [2]. Today it is called as the de Broglie matter wave.

An effort has made to generalize the de Broglie matter wave to planetary wave for a long time, but has faced many difficulties; traditional quantum theory cannot properly deal with some gravity problems [3][4][5]. In recent years, generalized relativistic matter wave has been proposed and applied to the solar system to explain quantum gravity effects, this approach provides a new method for quantum gravity. Consider a particle, its relativistic matter wave is given by

$$\psi = \exp(\frac{i\beta}{c^3}\int_0^x (u_1 dx_1 + u_2 dx_2 + u_3 dx_3 + u_4 dx_4)) \quad . \tag{1}$$

where u is the 4-velocity of the particle, β is the ultimate acceleration [6] determined by experiments. This paper show that the relativistic matter wave provides a biological clock for human beings, it also governs planetary size and temperature. As the results, the period of sunspot cycle is calculated as 10.93 years, the human lifespan on the Earth

is calculated to be 84 years, while the human lifespan reduces to 8.6 years on the Mars. The temperatures in the solar interior and in the earth's interior are also calculated by their relativistic matter waves.

2. Example 1: determining the solar ultimate acceleration β and radius

Bohr's orbital model as shown in Figure 1(a), the planetary circular orbit can be quantized in terms of the relativistic matter wave, the circumference is n multiple of the wavelength as follows

$$\left.\begin{aligned} \frac{\beta}{c^3}\oint_L v_l dl = 2\pi n \\ v_l = \sqrt{\frac{GM}{r}} \end{aligned}\right\} \Rightarrow \sqrt{r} = \frac{c^3}{\beta\sqrt{GM}} n; \quad n = 0,1,2,\ldots \ . \tag{2}$$

This orbital quantization rule only achieves a half success in the solar system, as shown in Figure 1(b), the Sun, Mercury, Venus, Earth and Mars satisfy the quantization equation; while other outer planets fail. But, since we only study quantum gravity effects among the Sun, Mercury, Venus, Earth and Mars, so this orbital quantization rule is good enough as a foundational quantum theory. In Figure 1(b), the blue straight line expresses a linear regression relation among the quantized orbits, so it gives β=2.961520e+10 (m/s^2). The quantum numbers n=3,4,5,... were assigned to the solar planets, the sun was assigned a quantum number n=0 because the sun is in the **central state**.

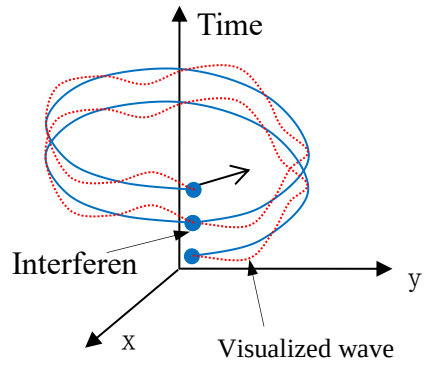

(a)

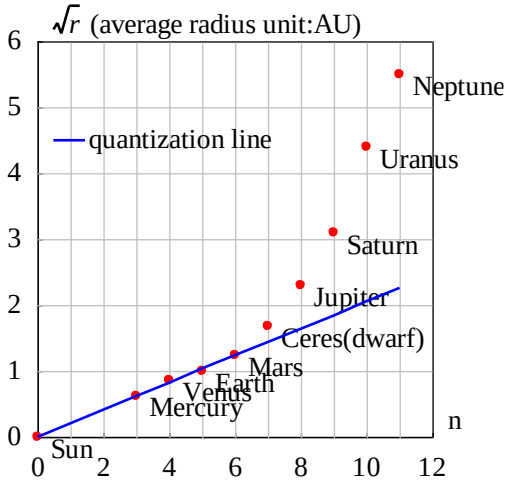

(b)

Figure 1 (a)The head of the relativistic matter wave may overlap with its tail. (b) The inner planets are quantized.

The relativistic matter wave can be applied to determine the solar density and radius.

In a central state, if the coherent length of the relativistic matter wave is long enough, its head may overlap with its tail when the particle moves in a closed orbit, as shown in Figure 1(a). The overlapped wave on the equatorial plane is given by

$$\psi = \psi(r)T(t)$$

$$\psi(r) = 1 + e^{i\delta} + e^{i2\delta} + \ldots + e^{i(N-1)\delta} = \frac{1-\exp(iN\delta)}{1-\exp(i\delta)} \quad . \tag{3}$$

$$\delta(r) = \frac{\beta}{c^3}\oint_L (v_l)dl = \frac{2\pi\beta\omega r^2}{c^3}$$

where N is the overlapping number which is determined by the coherent length of the relativistic matter wave, δ is the phase difference after one orbital motion, ω is the angular speed of the solar self-rotation. The above equation is a multi-slit interference formula in optics, for a larger N it is called as the Fabry-Perot interference formula.

The relativistic matter wave function ψ needs a further explanation. In quantum mechanics, $|\psi|^2$ equals to the probability of finding an electron due to Max Burn's explanation; in astrophysics, $|\psi|^2$ equals to the probability of finding a nucleon (proton or neutron) *averagely on an astronomic scale*, we have

$$|\psi|^2 \propto \text{nucleon-density} \propto \rho \quad . \tag{4}$$

It follows from the multi-slit interference formula that the overlapping number N is estimated by

$$N^2 = \frac{|\psi(0)_{multi-wavelet}|^2}{|\psi(0)_{one-wavelet}|^2} = \frac{\rho_{core}}{\rho_{surface\_gas}} \quad . \tag{5}$$

The solar core has a mean density of 1408 (kg/m^3), the surface of the sun is comprised of convective zone with a mean density of 2e-3 (kg/m^3) [7]. In this paper, the sun's radius is chosen at a location where density is 4e-3 (kg/m^3), thus the solar overlapping number N is calculated to be N=593.

Sun's angular speed at its equator is known as ω=2π/(25.05x24x3600) (s^{-1}). Its mass 1.9891e+30 (kg), well-known radius 6.95e+8 (m), mean density 1408 (kg/m^3), the constant β=2.961520e+10 (m/s^2). According to the N=593, the matter distribution of the $|\psi|^2$ is calculated in Figure 2, it agrees well with the general description of star's interior [8]. The radius of the sun is determined as r=7e+8 (m) with a relative error of 0.72% in Figure 2, which indicates that the sun radius strongly depends on the sun's self-rotation.

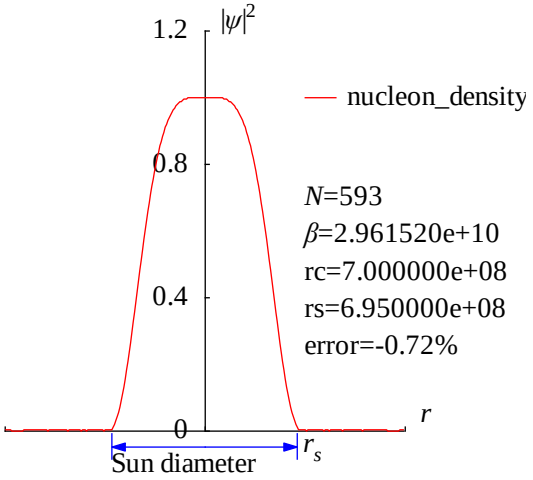

Figure 2 The nucleon distribution $|\psi|^2$ in the Sun is calculated in the radius direction.

```
<Clet2020 Script>//C source code [9]
int i,j,k,m,n,N,nP[10];
double beta,H,B,M,r,r_unit,x,y,z,delta,D[1000],S[1000], a,b,rs,rc,omega,atm_height; char str[100];
main(){k=150;rs=6.95e8;rc=0;x=25.05;omega=2*PI/(x*24*3600);n=0; a=1408/0.004; N=sqrt(a);
beta=2.961520e10;H=SPEEDC*SPEEDC*SPEEDC/beta;M=1.9891E30; atm_height=2e6; r_unit=1E7;
for(i=-k;i<k;i+=1) {r=abs(i)*r_unit;
if(r<rs+atm_height) delta=2*PI*omega*r*r/H; else delta=2*PI*sqrt(GRAVITYC*M*r)/H;//around the star
x=1;y=0; for(j=1;j<N;j+=1) { z=delta*j; x+=cos(z);y+=sin(z);} z=x*x+y*y; z=z/(N*N);
S[n]=i;S[n+1]=z; if(i>0 && rc==0 && z<0.0001) rc=r; n+=2;}
SetAxis(X_AXIS,-k,0,k,"#ifr; ; ; ;");SetAxis(Y_AXIS,0,0,1.2,"#if|ψ|#su2#t;0;0.4;0.8;1.2;");
DrawFrame(FRAME_SCALE,1,0xafffaf); z=100*(rs-rc)/rs;
SetPen(1,0xff0000);Polyline(k+k,S,k/2,1," nucleon_density"); SetPen(1,0x0000ff);
r=rs/r_unit;y=-0.05;D[0]=-r;D[1]=y;D[2]=r;D[3]=y; Draw("ARROW,3,2,XY,10,100,10,10,",D);
Format(str,"#ifN#t=%d#n#ifβ#t=%e#nrc=%e#nrs=%e#nerror=%.2f%",N,beta,rc,rs,z);
TextHang(k/2,0.7,0,str);TextHang(r+5,y/2,0,"#ifr#sds#t");TextHang(-r,y+y,0,"Sun diameter");
}#v07=?>A
```

3. Example 2: determining the earth's ultimate acceleration β and radius

The moon is assigned a quantum number of n=2 because some quasi-satellite's perigees have reached a depth almost at n=1 orbit, as shown in Figure 3. Here, the ultimate acceleration β=1.377075e+14(m/s^2) is determined uniquely by the line between the earth and moon by Eq. (2).

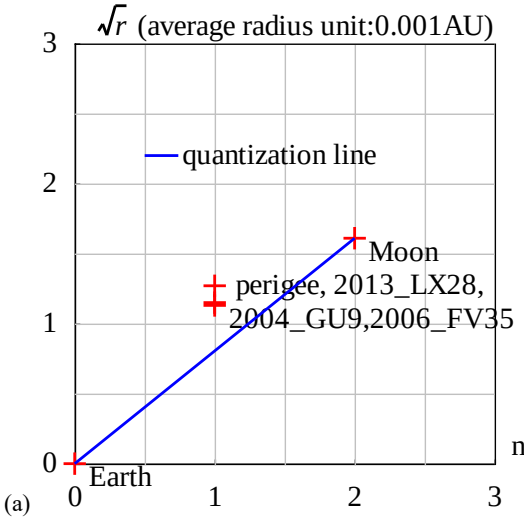

Figure 3 Orbital quantization for the moon.

The earth has a mean density of 5530 (kg/m^3), its surface is covered with air and vapor with a density of 1.29 (kg/m^3). The earth's radius is chosen at the sea level, it follows Eq.(5) that the earth's overlapping number N is calculated to be N=65.

The earth's angular speed is known as ω=2π/(24x3600) (s^{-1}), its mass 5.97237e+24 (kg), the well-known radius is 6.371e+6 (m), the earth's constant β=1.377075e+14 (m/s^2). The matter distribution $|\psi|^2$ in radius direction is calculated by Eq.(3), as shown in Figure 4(a). The radius of the earth is determined as r=6.4328e+6 (m) with a relative error of 0.86%, it agrees well with common knowledge. The secondary peaks over the atmosphere up to 2000 km altitude are calculated in Figure 4(b) which agree well with the space debris observations [10][11][12].

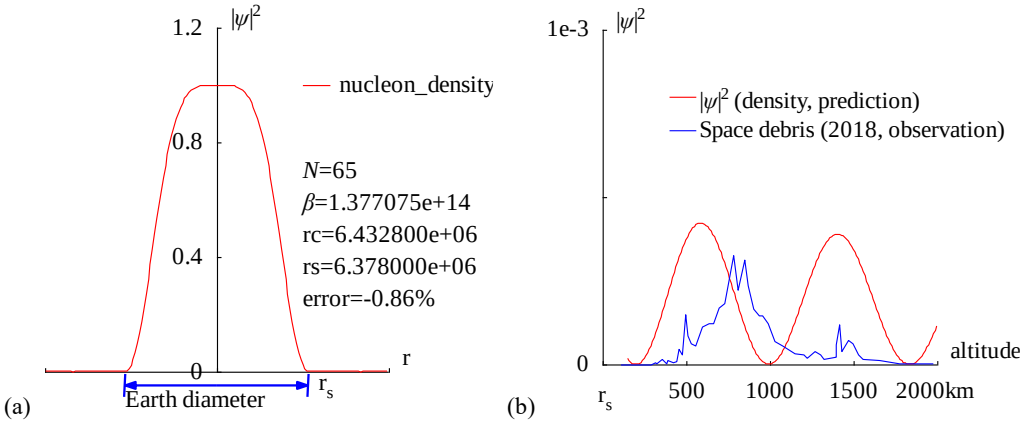

Figure 4 (a) The radius of the Earth is calculated out r=6.4328e+6 (m) with a relative error of 0.86% by the interference of its relativistic matter wave; (b) The prediction of the space debris distribution up to 2000 km altitude.

```
<Clet2020 Script>//C source code [9]
int i,j,k,m,n,N,nP[10]; double H,B,M,v_r,r,AU,r_unit,x,y,z,delta,D[10],S[1000];
double rs,rc,rot,a,b,atm_height,beta; char str[100];
main(){k=80;rs=6.378e6;rc=0;atm_height=1.5e5;n=0; N=65;
beta=1.377075e+14;H=SPEEDC*SPEEDC*SPEEDC/beta;
M=5.97237e24;AU=1.496E11;r_unit=1e-6*AU; rot=2*PI/(24*60*60);//angular speed of the Earth
for(i=-k;i<k;i+=1) {r=abs(i)*r_unit;
if(r<rs+atm_height) v_r=rot*r*r; else v_r=sqrt(GRAVITYC*M*r);//around the Earth
delta=2*PI* v_r/H; y=SumJob("SLIT_ADD,@N,@delta",D); y=y/(N*N);
if(y>1) y=1; S[n]=i;S[n+1]=y; if(i>0 && rc==0 && y<0.001) rc=r;   n+=2;}
SetAxis(X_AXIS,-k,0,k,"r; ; ; ;");SetAxis(Y_AXIS,0,0,1.2,"#if|ψ|#su2#t;0;0.4;0.8;1.2;");
DrawFrame(FRAME_SCALE,1,0xafffaf); x=50;z=100*(rs-rc)/rs;
SetPen(1,0xff0000);Polyline(k+k,S,k/2,1," nucleon_density");
r=rs/r_unit;y=-0.05;D[0]=-r;D[1]=y;D[2]=r;D[3]=y;
SetPen(2,0x0000ff); Draw("ARROW,3,2,XY,10,100,10,10,",D);
Format(str,"#ifN#t=%d#n#ifβ#t=%e#nrc=%e#nrs=%e#nerror=%.2f%",N,beta,rc,rs,z);
TextHang(k/2,0.7,0,str);TextHang(r+5,y/2,0,"r#sds#t");TextHang(-r,y+y,0,"Earth diameter");
}#v07=?>A#t
```

```
<Clet2020 Script>//C source code [9]
int i,j,k,m,n,N,nP[10]; double H,B,M,v_r,r,AU,r_unit,x,y,z,delta,D[10],S[10000];
double rs,rc,rot,a,b,atm_height,p,T,R1,R2,R3; char str[100]; int
Debris[96]={110,0,237,0,287,0,317,2,320,1,357,5,380,1,387,4,420,2,440,3,454,14,474,9,497,45,507,26,527,19,557,17,597,34,63
4,37,664,37,697,51,727,55,781,98,808,67,851,94,871,71,901,50,938,44,958,44,991,37,1028,21,1078,17,1148,10,1202,9,1225,6,
1268,12,1302,9,1325,5,1395,7,1395,18,1415,36,1429,12,1469,22,1499,19,1529,9,1559,5,1656,4,1779,1,1976,1,};
main(){k=80;rs=6.378e6;rc=0;atm_height=1.5e5;n=0; N=65;
H=1.956611e11;M=5.97237e24;AU=1.496E11;r_unit=1e4;
rot=2*PI/(24*60*60);//angular speed of the Earth
b=PI/(2*PI*rot*rs*rs/H); R1=rs/r_unit;R2=(rs+atm_height)/r_unit;R3=(rs+2e6)/r_unit;
for(i=R2;i<R3;i+=1) {r=abs(i)*r_unit; delta=2*PI*sqrt(GRAVITYC*M*r)/H;
y=SumJob("SLIT_ADD,@N,@delta",D); y=1e3*y/(N*N);// visualization scale:1000
if(y>1) y=1; S[n]=i;S[n+1]=y;n+=2;}
SetAxis(X_AXIS,R1,R1,R3,"altitude; r#sds#t;500;1000;1500;2000km ;");
SetAxis(Y_AXIS,0,0,1,"#if|ψ|#su2#t;0; ;1e-3;");DrawFrame(FRAME_SCALE,1,0xafffaf); x=R1+(R3-R1)/5;
SetPen(1,0xff0000);Polyline(n/2,S,x,0.8,"#if|ψ|#su2#t (density, prediction)");
for(i=0;i<48;i+=1) {S[i+i]=R1+(R3-R1)*Debris[i+i]/2000; S[i+i+1]=Debris[i+i+1]/300;}
SetPen(1,0x0000ff);Polyline(48,S,x,0.7,"Space debris (2018, observation) "); }#v07=?>A#t
```

4. Period of sunspot cycle

The **coherence length** of waves is usually mentioned but the **coherence width** of waves is rarely discussed in quantum mechanics, simply because the latter is not a matter for electrons, nucleon, or photons, but it is a matter in astrophysics. The analysis of observation data tells us that on the planetary scale, the coherence width of relativistic matter waves can extend to 1000 kilometers or more, as illustrated in Figure 5(a), the overlap may even occur in the width direction, thereby bringing new aspects to wave interference.

In the solar convective zone, adjacent convective arrays form a top-layer flow, a middle-layer gas, and a ground-layer flow, similar to the concept of **molecular current** in electromagnetism. Considering one convective ring at the equator as shown in Figure 5(b), there is an apparent velocity difference between the top-layer flow and the middle-layer gas, where their relativistic matter waves are denoted respectively by

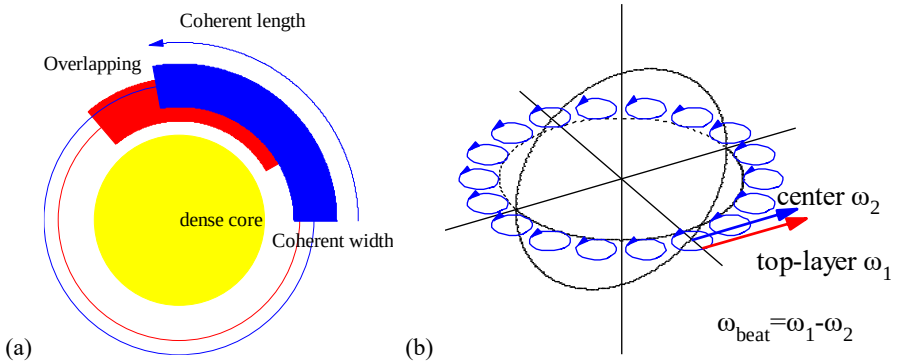

Figure 5 (a) Illustration of overlapping in the coherent width direction. (b) In convective rings at the equator, the speed difference causes a beat frequency.

$$\begin{aligned}
&\psi = \psi_{top} + C\psi_{middle} \\
&\psi_{top} = \exp[\frac{i\beta}{c^3}\int_L (v_1 dl + \frac{-c^2}{\sqrt{1-v_1^{\,2}/c^2}}dt)] \\
&\psi_{middle} = \exp[\frac{i\beta}{c^3}\int_L (v_2 dl + \frac{-c^2}{\sqrt{1-v_2^{\,2}/c^2}}dt)]
\end{aligned} \quad . \tag{6}$$

Their interference in the coherent width direction leads to a beat phenomenon

$$\begin{aligned}
&|\psi|^2 = |\psi_{top} + C\psi_{middle}|^2 = 1 + C^2 + 2C\cos[\frac{2\pi}{\lambda_{beat}}\int_L dl - \frac{2\pi}{T_{beat}}t] \\
&\frac{2\pi}{T_{beat}} = \frac{\beta}{c^3}(\frac{c^2}{\sqrt{1-v_1^{\,2}/c^2}} - \frac{c^2}{\sqrt{1-v_2^{\,2}/c^2}}) \simeq \frac{\beta}{c^3}(\frac{v_1^{\,2}}{2} - \frac{v_2^{\,2}}{2}) \\
&\frac{2\pi}{\lambda_{beat}} = \frac{\beta}{c^3}(v_1 - v_2); \quad V = \frac{\lambda_{beat}}{T_{beat}} = \frac{1}{2}(v_1 + v_2)
\end{aligned} \quad . \tag{7}$$

Their speeds are calculated as

$$\begin{aligned}
&v_1 \approx 6100\,(m/s) \quad (\approx \text{observed in Evershed flow}) \\
&v_2 = \omega r_{middle} = 2017\,(m/s) \quad (\text{solar rotation});
\end{aligned} \quad . \tag{8}$$

Where, regarding Evershed flow as the eruption of the top-layer flow, about 6 (km/s) speed was reported [13]. Alternatively, the top-layer speed v_1 also can be calculated in terms of thermodynamics, to be v_1=6244 (m/s) [6]. Here using v_1=6100 (m/s), their beat period T_{beat} is calculated to be a value of 10.93 (years), in agreement with the sunspot cycle value (say, mean 11 years).

$$T_{beat} \simeq \frac{4\pi c^3}{\beta\left(v_1^{\,2} - v_2^{\,2}\right)} = 10.93\,(years) \quad . \tag{9}$$

The relative error to the mean 11 years is 0.6% for the beat period calculation using the relativistic matter waves. This beat phenomenon turns out to be a **nucleon density oscillation** that undergoes to drive the sunspot cycle evolution. The beat wavelength λ_{beat} is too long to observe, only the beat period is easy to be observed. As shown in Figure 6, on the solar surface, the equatorial circumference $2\pi r$ only occupies a little part of the beat wavelength, what we see is the expansion and contraction of the nucleon density.

$$\frac{2\pi r}{\lambda_{beat}} = 0.0031 \quad . \tag{10}$$

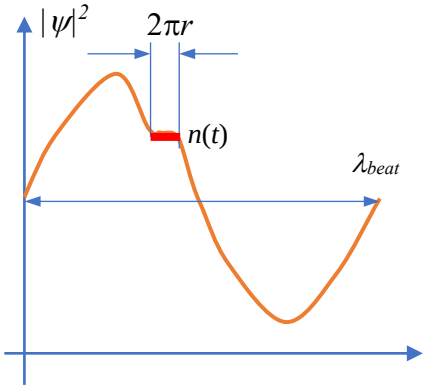

Figure 6 The equatorial circumference 2πr only occupies a little part of the beat wavelength, what we see is the expansion and contraction of the nucleon density.

This nucleon density oscillation is understood as a new type of nuclear reaction on an astronomic scale.

In the above calculation, although this seems to be a rough model, there is an obvious correlation between solar radius, solar rotation, solar density, and solar constant β.

5. Atmospheric circulation with season clock

Consider a relativistic matter wave ψ_A in the earth shell at the latitude angle A, it will interfere with its neighbor waves within its coherent width. Because the earth shell mainly consists of dense matter, their mutual cascade-interference will cause the relativistic matter waves to have spherical symmetry, so that the relativistic matter wave ψ_A at the latitude angle A should equal to the $\psi_{equator}$ at the equator, as shown in Figure 7(a). This property is supported by the spherical symmetry of the earth's density distribution:

$$\begin{aligned} &\text{spherical symmetry: } \rho(r, A, \varphi) = \rho(r) \quad \Rightarrow \quad \psi(r, A, \varphi) = \psi(r) \\ &\text{or: } \psi_A = \psi_{equator} \end{aligned} \quad . \tag{11}$$

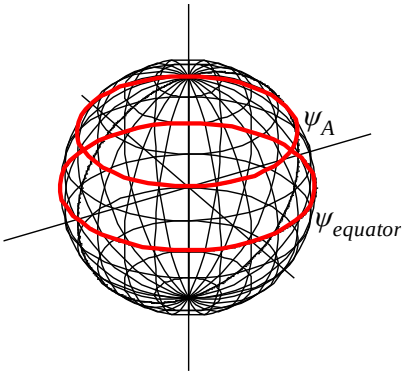

(a)

(b)

Figure 7 (a) Mutual cascade-interference will lead to the symmetry of the earth's density distribution. (b) Zonal winds on Jupiter (the photo from public News).

On the contrary, in the thin atmosphere, the wind and clouds are freely distributed in the sky on a large scale, because their cascade-interference within coherence width can be ignored.

Using the coherent width concept, considering the interference between the air ψ_A at the latitude angle A and the shell ψ_{shell} at the same latitude, their interference is

$$\begin{aligned}
&\psi(r,A) = \psi_{air}(r,A) + C\psi_{shell}(r,A) = \psi_{air}(r,A) + C\psi_{shell_equator}(r) \\
&T_{beat} \simeq \frac{4\pi c^3}{\beta\left(v_{shell_equator}{}^2 - v_{air}{}^2\right)} \quad . \qquad (12) \\
&v_{shell_equator} = \omega r \\
&v_{air} = \omega r\cos(A) + v_{wind} + v_{sun_effect}
\end{aligned}$$

where C represents the coupling constant which relates to their distance and mass fractions, their interference leads to a beat phenomenon. Positive wind defined as in the direction from west to east, the term v_{sun_effect} represents the action of the sun on the air. The beat phenomenon is characterized as follows.

(1) Forced Oscillation

Due to the tilt 23.5° of the earth axis with respect to the earth's orbital plane, the directly shined latitude A_1 sways within A=23.5°S ~ 23.5°N, for example, in spring the directly shined latitude is about at A_1=12°N on the northern hemisphere. The air at the directly shined latitude is subjected to the solar radiation which forces the beat oscillation to run at the period T_{beat}=1 (year), where air density varys.

(2) Calm at the directly shined latitude, zero wind

Where the air constructively interferes with the solar radiation. This directly shined latitude A_1 is called as the first constructive interference ridge. Substituting zero wind into the above beat period forma, with T_{beat}=1 (year), we obtain the sun effect at the ridge:

$$v_{sun\_effect} = 369.788 - \omega r\cos(A_1); \quad (units: m/s) \quad . \qquad (13)$$

At other latitude A we should introduce inclination factor for the solar radiation, the global sun effect be

$$v_{sun\_effect} = 369.788\cos(A - A_1) - \omega r\cos(A) \quad . \qquad (14)$$

(3) Wind formula

Calm at the ridge, while breeze winds nearby. Substituting the global sun effect into the above beat period forma, the wind under control of the beat T_{beat} nearby the ridge is given by

$$v_{wind} = \sqrt{\omega^2 r^2 - \frac{4\pi c^3}{\beta T_{beat}}} - \omega r \cos(A) - v_{sun\_effect} \quad . \tag{15}$$

It is not easy to maintain the constructive interference condition for these waves. When the first constructive interference ridge is at latitude A_1=12°N, the wind required for maintaining the beat T_{beat}=1 (year) nearby is calculated by the above equation as shown in Figure 8(a) (blue line).

(4) The second ridge and third ridge

As the latitude A rises, the first ridge will be destroyed by destructive interference, but, the waves will again satisfy the constructive interference condition at next locations. At A=39°N location (second ridge) where beat T_{beat}=0.5 (years), and at A=57°N location (third ridge) where beat T_{beat}=0.37 (years) which is the shortest period that the earth can get within the arctic regions. The winds nearby the second ridge and third ridge are shown in Figure 8(a).

(5) Wind-curve over the northern hemisphere

The maximal wind appears at the midpoint of the first two ridges, about 48 (m/s). Linking all characteristic points in Figure 8(a) we obtain the predicted wind-curve over the northern hemisphere; this prediction agrees well with the experimental observations at an altitude of 10km (200hPa) [14], as shown in Figure 9. The zonal winds on the Jupiter has the same characteristics, as shown in Figure 7(b).

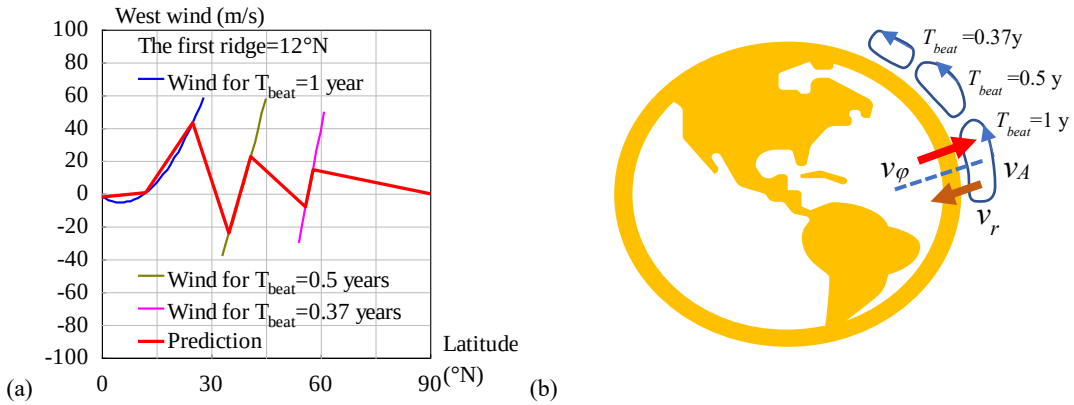

Figure 8 (a) Calculation of west winds in the northern hemisphere. (b) The atmospheric circulation in the northern hemisphere.

```
<Clet2020 Script>//C source code [9]
double beta,H,M,r,rc, rs, rot,v1,v2, Year,T,Lamda,V,a,b,w,Fmax,N[500],S[500],F[100]; int i, j, k, t, m, n, s, f,Type,x;
int main(){beta=1.377075e+14; H=SPEEDC*SPEEDC*SPEEDC/beta;
M=5.97237e24; rs=6.371e6; rot=2*PI/(24*3600); Year=24*3600*365.2422;
Type=1; x=10; if(Type>1) x=-30;//v2=rs*rot; a=v2*v2-4*PI*H/Year; V=sqrt(a)-v2;
if(Type==1)   SetAxis(X_AXIS,0,0,90,"Latitude#n(°N);0;30;60;90;");
else   SetAxis(X_AXIS,-90,-90,90,"Latitude#n(°N);=90;-60;-30;0;30;60;90;");
SetAxis(Y_AXIS,-100,-100,100,"West wind (m/s);-100;-80;-60;-40;-20;0;20;40;60;80;100;");
DrawFrame(0x016a,Type,0xafffaf);//Polyline(2,"-90,0,90,0");
Check(15,k); if(k>24) k=24; if(k<-24) k=-24; //TextAt(100,10,"V=%f",V);
T=Year/2; Wind(); f=0; Findf(); t=N[m+m]; T=Year; Wind(); f=0; Findf();
SetPen(2,0xff); Polyline(n,N,x,70,"Wind for T#sdbeat#t=1 year"); if(Type>1) Polyline(s,S);
F[0]=N[0];F[1]=N[1]; F[2]=N[m+m]; F[3]=N[m+m+1];   t=(t+F[2])/2;//midst of two ridges
  t=t-F[2]+m; Fmax=N[t+t+1]; //TextAt(100,20,"t=%d, Fmax=%f ",t,Fmax);
f=Fmax; Findf(); F[4]=N[m+m]; F[5]=N[m+m+1];
T=Year/2; Wind(); f=-Fmax/2; Findf(); t=m;f=Fmax/2; Findf();
SetPen(2,0x80ff00); Polyline(n,N,x,-50,"Wind for T#sdbeat#t=0.5 years"); if(Type>1) Polyline(s,S);
```

```
F[6]=N[t+t]; F[7]=N[t+t+1];    F[8]=N[m+m]; F[9]=N[m+m+1];
T=0.37*Year; Wind(); f=-Fmax/4; Findf(); t=m;f=Fmax/4; Findf();
SetPen(2,0x9933fa); Polyline(n,N,x,-70,"Wind for T#sdbeat#t=0.37 years"); if(Type>1) Polyline(s,S);
F[10]=N[t+t]; F[11]=N[t+t+1];    F[12]=N[m+m]; F[13]=N[m+m+1];    F[14]=90; F[15]=0;
//Draw("ELLIPSE,0,2,XYX,10","15,20,25,35");TextHang(5,40,0,"a route");
SetPen(3,0xff0000); Polyline(8,F,x,-90,"Prediction"); TextHang(x,90,0,"The first ridge=%d°N", k);
}
Wind(){n=0;s=0;
for(i=0;i<90;i+=1)    { a=i*PI/180; b=(i-k)*PI/180; v1=rot*rs*cos(a); v2=rot*rs;
w=369.788*cos(b)-v2*cos(k*PI/180); a=v2*v2-4*PI*H/T; V=sqrt(a)-v1-w;
if(V>-40 && V<60) {N[n+n]=i; N[n+n+1]=V; n+=1;}}
for(i=0;i<90;i+=1)    { a=-i*PI/180; b=(-i-k)*PI/180; v1=rot*rs*cos(a); v2=rot*rs;
w=369.788*cos(b)-v2*cos(k*PI/180); a=v2*v2-4*PI*H/T; V=sqrt(a)-v1-w;
if(V>-40 && V<60) {S[s+s]=-i; S[s+s+1]=V; s+=1;}} }
Findf(){a=1e10; for(i=0;i<n;i+=1)    { b=N[i+i+1]-f ;if(b<0) b=-b;if(b<a) {m=i;a=b;}}
}//if(k==12) ClipJob(APPEND,"i=%d,V=%f",i,V);
#v07=?>A
```

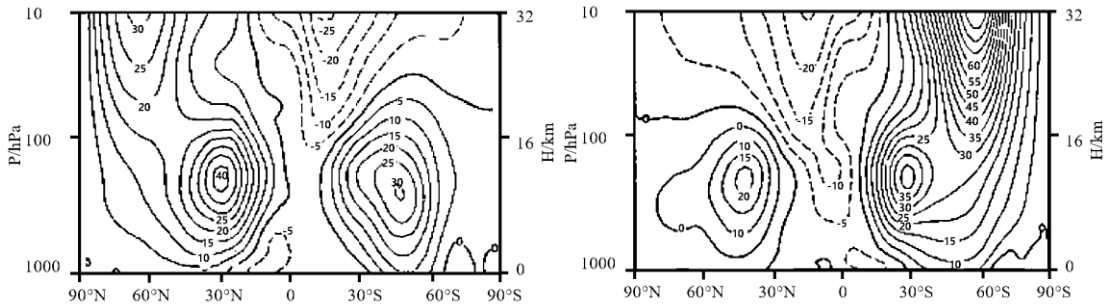

(a) (b)

Figure 9 NCEP/NCAR data, mean west winds over 40 years (1958~1997) [14]. (a) winter; (b) summer.

(6) Wind vector over the northern hemisphere

For further improvement of precision, the value of the wind should be resolved into three components in the spherical coordinates (r,A,φ) as

$$v_{wind}{}^2 = v_r{}^2 + v_A{}^2 + v_\varphi{}^2 \quad . \tag{16}$$

According to the energy equipartition theorem in thermodynamics, approximately we have their average estimation

$$< v_r{}^2 >=< v_A{}^2 >=< v_\varphi{}^2 >= \frac{1}{3} v_{wind}{}^2 \quad . \tag{17}$$

Thus, the wind vectors over the northern hemisphere of the Earth are plotted in Figure 8(b), where the atmospheric circulation consists of three cells: Hadley cell, Ferrel cell, and arctic cell.

(7) Season clock

The beat T_{beat}=1 (year) works out **two seasons** (dry and rainy) in the tropic regions. The beat T_{beat}=0.5 (years) blows comfortable winds over Europe, Northern America and Northeastern Asia, and modulates out **four seasons** (spring, summer, autumn, winter), this beat is a well-known **season clock**. The arctic regions favor well-quantized beat T_{beat}=1/3 (years) rather than the beat T_{beat}=0.37 (years), this situation gives rise to extra cold streams. The shortest beat T_{beat}=0.37 (years) has to adapt to the beat T_{beat}=1/3 (years) while emitting extra cold streams per 2.24 years to Europe, Northern America and Northeastern Asia [15], which are recognized as the **planetary scale waves** or **Rossby waves**.

(8) Easterlies at the equator

Since the relativistic matter wave of the air interferes with the relativistic matter wave

of the earth shell, the easterlies at the equator have a magnitude of about 10 m/s in Figure 8(a). The trade winds or the easterlies are the permanent east-to-west **prevailing winds** that flow in the Earth's equatorial region.

6. Human biological clock

Human body consists of five parts: one head and four limbs, a heart pumps the blood to the whole body circularly. Consider a person sleeping in a bed with the head pointing to the North Pole, as shown in Figure 10(a), the five red lines from the heart represent its five artery tubes.

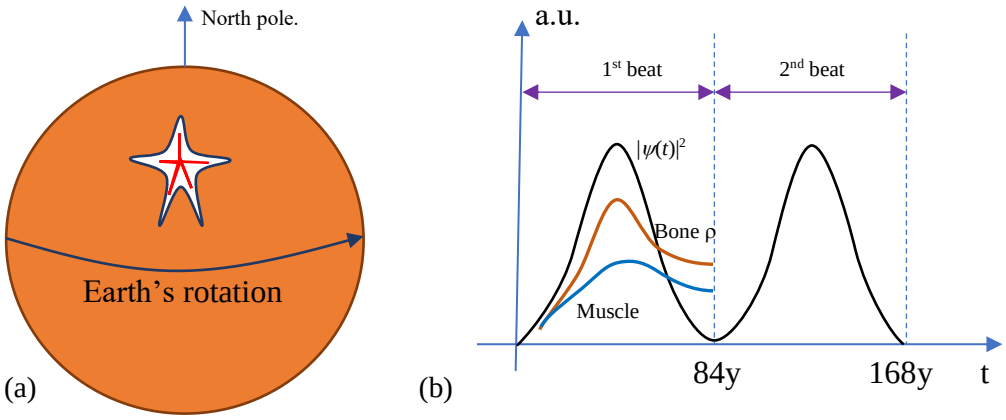

Figure 10 (a)A human sketch with the head pointing to the North Pole. (b) the biological clock.

Apparently, the arterial blood flows into the two arms with a speed, whose matter wave would interfere with the Earth's shell matter wave, producing a beat phenomenon:

$$|\psi|^2=|\psi_{blood}+C\psi_{shell}|^2=1+C^2+2C\cos[\frac{2\pi}{\lambda_{beat}}\int_L dl-\frac{2\pi}{T_{beat}}t]$$
$$\frac{2\pi}{T_{beat}}=\simeq\frac{\beta}{c^3}(\frac{v_{blood}^{\ 2}}{2}-\frac{v_{shell}^{\ 2}}{2});\quad \frac{2\pi}{\lambda_{beat}}=\frac{\beta}{c^3}(v_{blood}-v_{shell});\quad v_{shell}=\omega r \qquad (18)$$

where C represents the coupling coefficient, ω is the Earth's angular speed, r the Earth radius, shell's ψ_{shell} is with spherical symmetry. The blood flow velocity varies with the location of blood vessels. The normal value of aortic valve orifice blood flow velocity in adults is 1.0-1.7m/s, and that in children is 1.2-1.8m/s. The flow velocity of carotid artery is less than 1.2m/s, the normal flow velocity of abdominal aorta is less than 1.8 m/s, and the normal flow velocity of inferior vena cava is 0.05-0.25m/s. So, 1m/s is the order of magnitude of the blood velocities. Suppose the mean blood speed in human arms is 1m/s near the heart, then the flowing blood suffers a beat with the period as the follows

$$v_{shell}=r\omega=463.8m/s;\quad v_{blood}=v_{shell}\pm 1m/s$$
$$T_{beat}\simeq\frac{4\pi c^3}{\beta\left(v_{blood}^{\ 2}-v_{shell}^{\ 2}\right)}=\pm 84\,(years);\quad \lambda_{beat}=1.2e+12(m) \qquad (19)$$

<Clet2020 Script>// [9]
double beta,H,M,r,rc, rs, rot,v1,v2, Year,T,Lamda,V,a,b,x,y,w;

```
int main(){beta=1.377075e+14; H=SPEEDC*SPEEDC*SPEEDC/beta;
M=5.97237e24; rs=6.378e6; rot=2*PI/(24*3600); Year=24*3600*365.2422;
v1=rot*rs;v2=v1+1; a=v2*v2-v1*v1; T=4*PI*H/a;
T/=Year; Lamda=2*PI*H/(v2-v1); b=Lamda/(2*PI*rs);
TextAt(100,20,"v1=%f, v2=%f, T=%f, L=%e, b=%e",v1,v2,T,Lamda,b);
}#v07=?>A
```

In the fact, the blood is pumped from the heart into both the eastern arm and western arm in Figure 10(a), producing a positive beat and a negative beat in the two arms with the same period 84 years, the two beats form an overall beat through the two arms. It is found that human mean lifespan is just confined within the single period duration, this beat period is recognized as the **human biological clock**. The beat wavelength λ is 30000 times the circumference of the earth, so its λ effects are hardly observed.

According to the explanation to ψ in the preceding section, the beat $|\psi|^2$ represents the probability of finding a nucleon on a macro-scale, in other words, the $|\psi|^2$ is proportional to the matter density.

$$|\psi|^2 \propto \rho \ . \tag{20}$$

The $|\psi|^2$ oscillation of the beat in Figure 10(b) represents the variation of a human body density in his whole life confined within one beat period. The human bone density (red line) and muscle (blue line) in a human life vary as function of age, also responding to the $|\psi|^2$ oscillation, as shown in Figure 10(b). After astronauts entered the space station, the coupling between the astronauts and the earth's rotation decreased, and there was a significant decrease in bone density, indicating that the bone density of normal people on the earth's surface was strongly related to $|\psi|^2$.

Obviously, the human bone and muscle are irreversible for the life process, they also completely resist the human to enter into the second beat for obtaining a 168 years longevity. Perhaps, some soft animals or cells may enter multi-beat process for a longer life or immortal. Sleep position, walking, running, sitting, etc. may make influences on the human biological clock in some extent, cannot stop ticking of the human biological clock, because the blood never stops as the life. Human life process is accumulated by many instantaneous activities, so the accumulation formula for calculating human lifespan T is

$$\int_0^T \frac{F(C)dt}{T_{beat}(t)} = \int_0^T \frac{F(C)\beta\left(v_{blood}{}^2 - v_{shell}{}^2\right)}{4\pi c^3} dt = 1 \ . \tag{21}$$

Where $F(C)$ is a function of the instantaneous coupling coefficient C.

This formula can also be used to estimate animal lifespan. Wikipedia lists some long-lived creatures in the entry of " List of longest-living organisms " [16], for example, Harriet, a Galápagos tortoise, died at the age of 175 years in June 2006. Lin Wang, an Asian elephant, was the oldest elephant in the Taipei Zoo, he died on February 26, 2003 at 86 years. The oldest goat was McGinty who lived to the age of 22 years and 5 months until her death in November 2003 on Hayling Island, UK. The Greenland shark had been estimated to live to about 200 years. A goldfish named Tish lived for 43 years after being won at a fairground in 1956. Geoduck, a species of saltwater clam native to the Puget Sound, have been known to live more than 160 years. The longevity formula in this paper can cover these longevity animal examples.

7. How to understand physical effects of the relativistic matter wave

We can understand the physical effect of the $|\psi|^2$ from three aspects. (1) How do biological cells perceive $|\psi|^2$? As we know, $|\psi|^2$ represents the probability of finding nucleon on the macro scale. It can be likened to a balloon, as shown in Figure 11. The three black dots on the balloon represent three molecules of a biological cell. When the balloon or the ψ expands, the space between the three molecules of the biological cell becomes larger, thus weakening the binding force between them. When the balloon or the ψ shrinks, the space between the three molecules of the biological cell becomes smaller, so that the binding force between them increases. Therefore, biological cells can sense the physical changes of the ψ.

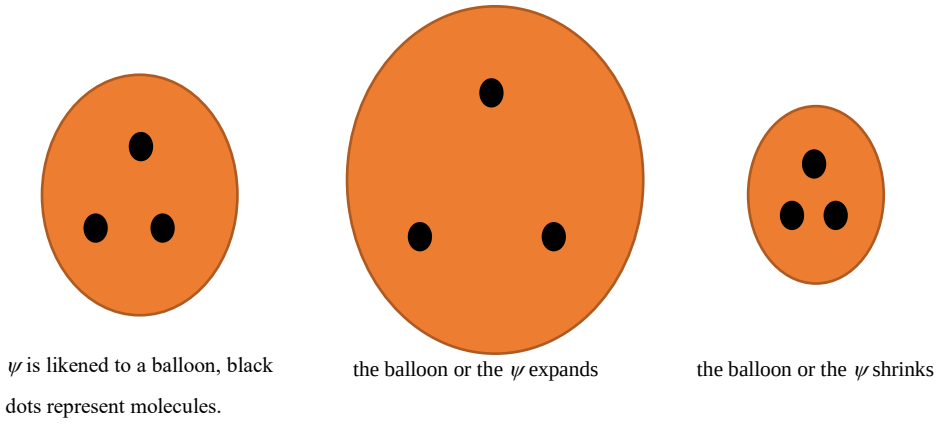

Figure 11 The ψ as if a balloon, the three dark dots represent tree molecules of a biological cell.

(2) Statistical characteristics of ψ. The section "Atmospheric circulation with season clock" points out that wind is a quantum gravity effect. If we observe our daily life, we will see a gust of wind, another gust of wind, and the performance is impermanent. However, the US NCEP/NCAR has proved that there is a fixed wind field on the earth's surface through 40 years of long-term observation, as shown in Figure 9. Therefore, wind is a quantum gravity effect seen in statistics. Similarly, the biological clock is also a quantum gravity effect seen in statistics. (3) ultimate velocity c and ultimate acceleration β. In the theory of relativity, the speed of light c is the ultimate velocity. As shown in Figure 12, the particle velocity v_1 observed in the experiment along the x_1 axis is the projection of the ultimate velocity ic (imaginary number) on the x_1 axis. Similarly, the particle acceleration a_1 observed in the experiment along the x_1 axis is the projection of the ultimate acceleration $i\beta$ (imaginary number) on the x_1 axis. In the figure, the ultimate velocity c and ultimate acceleration β form a solenoid "spring", and the relativistic material wave is the "elastic wave" of this abstract "spring" [6].

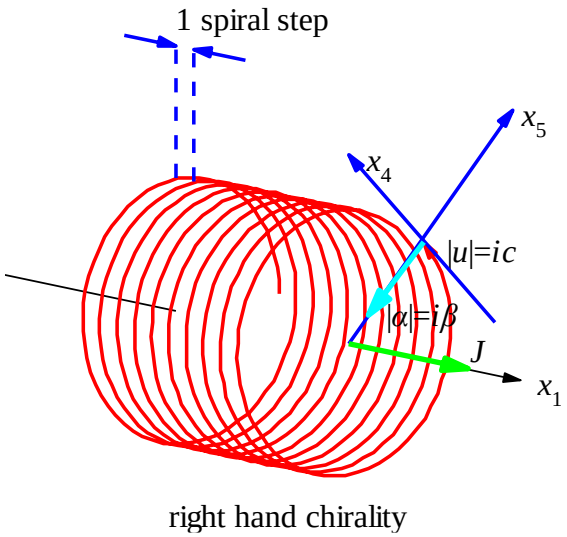

Figure 12 The particle moves along the x_1 axis with the constant speed $|u|=ic$ in u direction and constant centripetal force in the x_5 axis at the radius iR (imaginary number).

8. How 2D matter wave to obtain spin and convective layer

Dimension is defined as the number of independent parameters in a mathematical space. In the field of physics, dimension is defined as the number of independent space-time coordinates. 0D is an infinitesimal point with no length. 1D is an infinite line, only length. 2D is a plane, which is composed of length and width. 3D is 2D plus height component, has volume.

In this section we at first discuss how to measure dimension by wave. In Figure 13(a), one puts earphone into ear, one gets 1D wave in the ear tunnel.

$$1D: \quad y = A\sin(kr-\omega t) = \frac{A}{r^0}\sin(kr-\omega t)\cdot \tag{22}$$

where r is the distance between the wave emitter and the receiver. In Figure 13(b), one touches a guitar spring, one gets 2D cylinder wave.

$$2D: \quad y = \frac{A}{r^{1/2}}\sin(kr-\omega t)\cdot \tag{23}$$

In Figure 13(c), one turns on a music speaker, one gets 3D spherical wave.

$$3D: \quad y = \frac{A}{r}\sin(kr-\omega t)\cdot \tag{24}$$

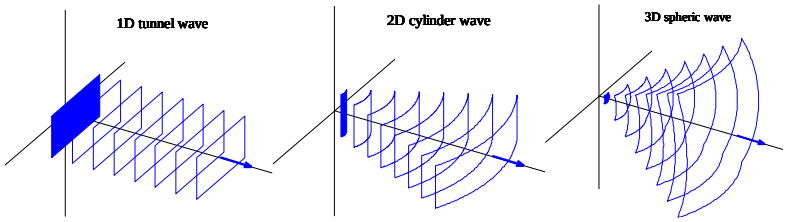

(a) 1D tunnel wave (b) 2D cylinder wave (c) 3D spherical wave

Figure 13 The wave behavior in various dimensional spaces.

<Clet2020 Script>// [9]
int i,j,k,type,nP[10]; double D[20],S[1000];
int main(){SetViewAngle("temp0,theta60,phi-30");SetAxis(X_AXIS,0,0,200,"X;0;200;");
DrawFrame(FRAME_LINE,1,0xafffaf); type=2;SetPen(1,0x00ff);

```
for(i=10;i<160;i+=20){D[0]=i;D[1]=0;D[2]=0;D[3]=i+5;D[4]=0;D[5]=0;D[6]=i;D[7]=10;D[8]=0;
if(type==0) {D[9]=4;D[10]=40;D[11]=20;D[12]=i;TextHang(50,0,100,"1D tunnel wave");k=CARD;}
else if(type==1) {D[9]=200;D[10]=i/2;D[11]=20;D[12]=i;TextHang(50,0,100,"2D cylinder wave");k=50;}
else {D[9]=200;D[10]=i/2;D[11]=i/2;D[12]=i;TextHang(50,0,100,"3D spheric wave");k=40;}
Lattice(k,D,S);nP[0]=POLYGON;nP[1]=0;nP[2]=200;nP[3]=XYZ;
if(i==10) nP[1]=3; if(type==0) nP[2]=4; Plot(nP,S[9]);}
j=30;D[3]=D[0]+j*S[0];D[4]=D[1]+j*S[1];D[5]=D[2]+j*S[2];
SetPen(3,0x00ff);Draw("ARROW,0,2,XYZ,10",D);}
#v07=?>A
```

In general, we can write a wave in the form

$$y = \frac{A}{r^w}\sin(kr - \omega t)\,. \tag{25}$$

It is easy to get the dimension of the space in where the wave lives, the dimension is D=2w+1. Nevertheless, wave can be used to measure the dimension of space, just by determining the parameter w.

Waves all contain a core oscillation (vibration invariance. Hubble's law not only tells us about redshift, but also clarifies the real situation in a sense: vibration invariance.)

$$\frac{d^2y}{dr^2} + k^2 y = 0\,, \tag{26}$$

Substituting y into the core oscillation, we obtain the radial wave equation

$$\frac{d^2y}{dr^2} + \frac{2w}{r}\frac{dy}{dr} + (k^2 + \frac{w(w-1)}{r^2})y = 0\,. \tag{27}$$

This equation expresses the wave behavior modulated by the spatial dimension parameter w. For 1D wave w=0, it is trivial, but for 2D wave w=1/2, it reduces to the Bessel equation in a cylinder coordinate system (r,φ)

$$\frac{d^2y}{dr^2} + \frac{1}{r}\frac{dy}{dr} + (k^2 - \frac{1}{4r^2})y = 0 \quad \text{(2D wave)}$$

comparing to the Schrodinger's equation: . (28)

$$\frac{d^2R(r)}{dr^2} + \frac{2}{r}\frac{dR(r)}{dr} + [k^2 - \frac{l(l+1)}{r^2}]R(r) = 0$$

In quantum mechanics, y is an electronic wave function, comparing to the Schrodinger radial wave equation in textbooks, we find that the -1/4r^2 term represents the electronic spin effect. However, here according to the above radial Bessel equation we can simply conclude that sound wave, electromagnetic wave, or any wave can have spin effect in 2D space! Let us use $\boldsymbol{k}$ denote the wave-vector, then the above 2D wave equation tells us

$$k_r^{\,2} = k^2 - k_\varphi^{\,2}; \quad k = \frac{2\pi}{\lambda}; \quad k_\varphi = \pm\frac{1}{2r}\,. \tag{29}$$

The k_φ causes the 2D wave-vector $\boldsymbol{k}$ to spin little by little as illustrated in Figure 14. The positive and negative k_φ corresponds to spin up and spin down respectively; as r goes to the infinity, the spin effect vanishes off.

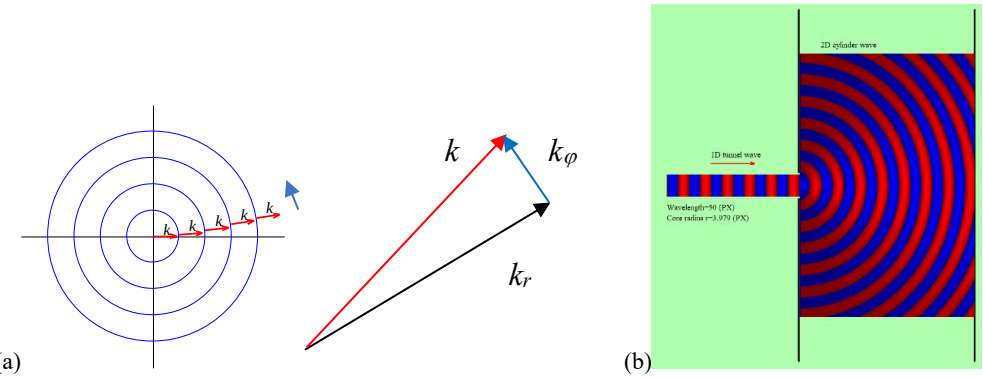

(a) (b)

Figure 14 (a) 2D wave-vector k spins little by little in the cylinder coordinates (r,φ). (b) from 1D to 2D, the spin works to split the electron beam due to double-value k_φ.

```
<Clet2020 Script>// Clet is a C compiler [26]
int i,j,k;double r,x,y,a,D[100];
int main(){DrawFrame(FRAME_LINE,1,0xafffaf); SetPen(1,0x0000ff);
for(i=0;i<90;i+=20) {D[0]=-i;D[1]=-i;D[2]=i;D[3]=i; Draw("ELLIPSE,0,2,XY,0",D);}
for(i=0;i<90;i+=20) {a=0.2*(i-i*i/200)*PI/180;r=i;D[0]=r*cos(a);D[1]=r*sin(a);
r+=18;D[2]=r*cos(a);D[3]=r*sin(a); SetPen(2,0xff0000);
Draw("ARROW,0,2,XY,8",D);TextHang(D[2]-10,D[3]+5,0,"#ifk");}
}#v07=?>A
```

If the 2D wave is the de Broglie matter wave for a particle beam, in a cylinder coordinate (r,φ), then the matter wave has a spin angular momentum given by

$$k_r = \frac{p_r}{\hbar}; \quad k_\varphi = \frac{p_\varphi}{\hbar} = \frac{J_\varphi}{r\hbar}; \quad J_\varphi = \pm\frac{1}{2}\hbar. \tag{30}$$

According to the angular momentum formula in general physics, it is recognized that the particle total momentum p is a constant given by

$$\left(\frac{p}{\hbar}\right)^2 = \left(\frac{p_r}{\hbar}\right)^2 + \left(\frac{p_\varphi}{\hbar}\right)^2. \tag{31}$$

$$k^2 = k_r^{\,2} + k_\varphi^{\,2} = const.$$

Since the particle total wave vector k is a constant, the wave-vector k_r must vary as r changes. The wave-vector in the radial direction would change as the wave attenuates.

Most physicists obtain redshift information from the Hubble law, but few physicists may think that the Hubble law implies invariance of wavelength on the solar-size scale, called as the vibration invariance. Consider a 2D matter wave emitting from a source with the wave vector $k=2\pi/\lambda$, there is a critical radius r_u where

$$k_r\big|_{r=r_u} = 0; \quad k_\varphi = \frac{1}{2r_u} = k = \frac{2\pi}{\lambda}; . \tag{32}$$

Within the area $r< r_u$, we deduce that $k_r=0$; while the outside area $r> r_u$, we deduce that k_r gradually grows as r grows until its spin component vanishes, crossing the boundary $r= r_u$ gives rise an uncertainty: left-hand spin or right-hand spin. Thus, the critical radius r_u is called the **uncertainty radius**, the area within $r< r_u$ is called the **uncertainty core**.

Due to some mechanism, suppose the left-hand spin retains, as illustrated in Figure 15(a). At the first, it is found that the wave progression in r direction within the uncertainty core is banned, that is $k_r=0$ because of $k_\varphi =k$, showing a vortex structure;

Next, if few matters leaking from the core spread out, they will bring away an amount of angular momentum from the source. For a stationary source, the leakage of angular momentum must be banned, on the boundary of the uncertainty radius, a convective array would form with which the wave progression erupts out from the gap of the convective array, in this case the convective array recycles almost all angular momentum leaked, as illustrated in Figure 15(b). The third, the circular component k_φ within the uncertainty core must be in a superfluid state, otherwise it will die in a shorter time due to dissipative motion, the uncertainty core must be a quantum superfluid vortex.

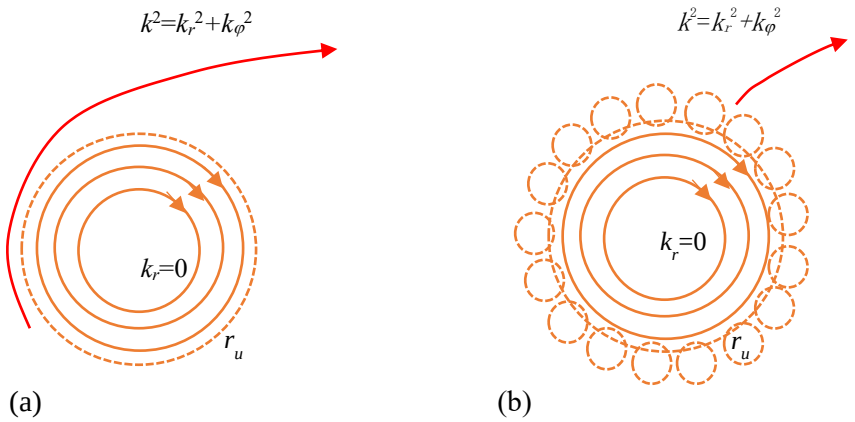

Figure 15 (a) The wave progression brings away an amount of angular momentum from the source, must be banned. (b) The convective array recycles almost all angular momentum leaked.

9. Temperature distribution in the sun and the earth

Now come back to astrophysics where relativistic matter waves govern all quantum gravity effects. For resisting the leakage of angular momentum due to the emission or absorption of relativistic matter waves on the solar system 2D plane, both the Sun and Earth have self-rotation and have convective zone in atmosphere, as shown in Figure 15(b).

During the formation of the circular vortex within the uncertainty core, the gas has to experience a dimension change from 2D to 1D circular motion, the gas has to redistribute its kinetic energy to support the circular flow, the motion in r direction must vanish in the way as follows

$$2D\begin{cases} E_\theta = \frac{1}{2}mv_\varphi^{\,2} \quad \Rightarrow \quad E_{\varphi\_thermal} \\ E_r = \frac{1}{2}mv_r^{\,2} \quad \Rightarrow \quad E_{\varphi\_flow} \end{cases}. \tag{33}$$

The thermal kinetic energy in the φ direction retains; while thermal kinetic energy in the r direction transforms into the circular flow energy (suppose the left-hand spin retains). According to the energy equipartition theorem, the flow speed of the gas can be used to estimate the temperature of the gas, that is

$$\frac{1}{2}kT=\frac{1}{2}mv_{flow}{}^{2}\quad\Rightarrow\quad T=\frac{mv_{flow}{}^{2}}{k}. \tag{34}$$

where m is the mean mass of the gas molecules, v_{flow} is the mean speed of the gas circular flow, k is the Boltzmann constant. In practice, in one hand, this 2D plane model would be applied to 3D situation which seem to comply with similar equation; in another hand, many circular quantum vortices may develop into different stages and be regarded as mature or immature, therefore, we have to introduce a compliance coefficient ξ so that this temperature formula is modified as

$$T=\xi\frac{mv_{flow}{}^{2}}{k}. \tag{35}$$

For a mature 2D vortex, its compliance coefficient ξ is 1; for a 3D immature situation, ξ<1.

Consider the sun, the solar surface is covered with adjacent convective arrays. Where, regarding the Evershed flow as the eruption of the top-layer flow of the convective zone, about 6000m/s speed was reported [13]. The solar atmosphere consists of 73.46% hydrogen atoms and 24.85% helium atoms. Thus, the compliance coefficient takes at ξ=0.8, and v_{flow}=6000m/s, the convective zone is estimated at a temperature T=6031K.

$$\begin{aligned} &m\approx 0.7346m_{hydrogen}+0.2485m_{helium};\\ &\xi=0.8;\quad v_{flow}=6000m/s;\quad T=6031K \end{aligned}. \tag{36}$$

```
<Clet2020 Script>//[9]
double v,m,T1,T2,v1,v2,rot,r,rs,Compliance; int i,j;
// Sun, Moon, Mercury, Venus, Earth, Mars, Jupiter,Saturn,Uranus,Neptune,
double Radius[10]={1.08968e2,0.27249,0.3825,0.9488,1,0.53226,11.209,9.449,4.007,3.883,}, R=6.378e6;//E
double Rotation[10]={25.05,27.32,58.6462,243.0187,0.99727,1.0259583,0.41354,0.444,0.7183,0.67125,};//day
double GasElement[10]={1.7286,1,1,1, 28,44,1,1,1,1,};//MP
double CoreElement[10]={1.7286,56,56,56, 56,56,1,1,1,1,};//MP
main(){ rs=6.378e6; j=100;
for(i=0;i<10;i+=1) { m=GasElement[i]*MP;rot=2*PI/(Rotation[i]*24*3600); r=Radius[i]*rs;
v1=rot*r; Compliance =0.4; if(i==0) {v1=6000; Compliance =0.8;}
T1= Compliance *m*v1*v1/BOLTZMANN; m=CoreElement[i]*MP;
v2=rot*r; T2=m*v2*v2/BOLTZMANN;
TextAt(100,j,"i=%d, T1=%f, T2=%f, v1=%f, v2=%f, ",i,T1,T2,v1,v2);
j+=50;}}#v07=?>A
```

This result agrees approximately with observation 5700K. Inside the sun, the solar core shell speed is given by $v_{flow}=r\omega$=2017m/s, the shell with ξ=1 is estimated with a temperature T=852K; in vicinity of the core center, the temperatures are estimated as 0K theoretically due to the dramatical drop of the rotating speed in the core. Why the center of the sun has a lower temperature? The sun acts as a quantum superfluid vortex, finally maintaining the same angular speed ω so that the center flow has a lower speed and at a lower temperature. We are sorry for the conclusion that the sun is neither a fireball glowing inside or a permanent energy reservoir.

Consider the earth, its atmosphere is composed of weaker convective arrays, if its vortex compliance coefficient takes ξ=0.4, then the atmospheric temperature at the sea level in the equatorial region is estimated to be T=293K.

$$\begin{aligned} m &\approx 28m_{hydrogen}; \quad \xi = 0.4; \\ v_{flow} &= r\omega = 465m/s; \quad T = 293K \end{aligned} \tag{37}$$

This result agrees approximately with observation at the equatorial area. Inside the earth, the mantle under the atmosphere is mainly composed of iron with a speed given by $v_{flow}=r\omega$=465m/s, the mantle temperature with ξ=1 is estimated to be T=1467K; in vicinity of the core center, the temperatures are estimated as 0K theoretically due to the dramatical drop of the rotating speed in the core.

The Moon, Mercury and Venus, have the similar characteristics. Among them, the wave vector k_r=0 in the uncertainty core of a quantum superfluid vortex causes the difficulty to transport heat to outside in the radial direction, while the energy exchange in the φ direction is under control of the winding relativistic matter waves, similar to the irrigation in circular fields in Figure 16.

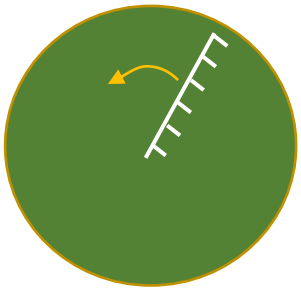

Figure 16 Similar to the irrigation in circular fields, the energy exchange in the φ direction is under control of the winding relativistic matter waves.

10. Guidance of anti-ageing

In the preceding section, we have derived the formula of human biological clock, consequently, increasing mean blood speed near human heart will lead to life reduction; decreasing mean blood speed near human heart will lead to life extension; the instantaneous coupling coefficient C is also an important factor. For pursuing life extension or anti-ageing, some ideas are devised as follows.

(1) Sleeping position

At the first, the head should point to the North Pole so that the projection component of the blood velocities in various parts of the body in the direction of the earth's rotation has a relatively small value which favor the life extension. Next, lying on a side also reduces the projection component of the blood velocities in the direction of the earth's rotation, comparing to the lying-stretched out, as illustrated in Figure 17(a).

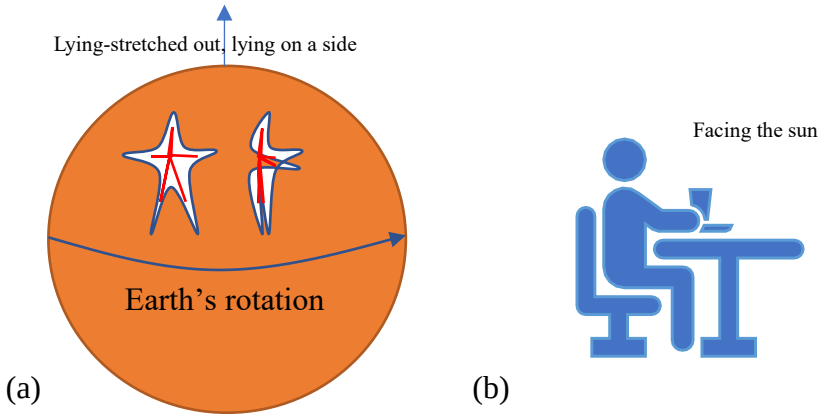

Figure 17 Lying-stretched out, lying on a side with the head pointing to the North Pole.

(2) Medicines

No doubt, some medicines can adjust the blood velocities in various parts of the human body. Normally, drinking tea, coffee, alcohol, etc. can increase the speed of blood in the human body for a while, leading to an accumulated effect for reducing the lifespan. Hydrophilic compounds such as alum can decease blood velocities in various parts of the body, but they are also appearing side and toxical effects for life bodies such as dementia.

More oxygen can reduce respiratory rate and blood flow speed, the higher the altitude, the thinner the oxygen, so residents living at low altitude live longer than residents living at high altitude. For example, China's statistics in 2021 show that the average life expectancy of the coastal city of Shanghai is 84.11 years [17]; The life expectancy of Qinghai Province in plateau area is 73.97 years [18], and that of Yunnan Province in plateau area is 74.4 years [19]. Vascular stent can significantly increase pore size and reduce blood flow speed. From January 2021 to November 2022, the purchase volume of coronary stents collected nationwide was 4.98 million [20], which was used in large cities such as Beijing and Shanghai. The relationship between this and the longevity of residents in large cities needs to be closely observed.

As we known, some Chinese traditional herbs can decease human blood velocities with less toxical effects, actually ancient Chinese didn't know how the herbs to work scientifically, today we get it based on the human biological clock.

(3) Office time

In china, office workers such as programmers, clerks, teachers, etc. spend 8 hours a day in offices. For weakening the coupling effects between blood velocities in human body and the earth's rotation for human life extension, workers need face the sun (east or west) when sitting for several hours, as illustrated in Figure 17(b). It is also suggested for the workers to drink cold-water and eat cold-foods.

(4) Architecture and environment

Almost all people spend their lives in rooms or buildings, architecture and environment have great impact on human lifetime. Many efforts in accordance with the quantum gravity theory [21] [22] are required to be made so that these architectures and environments benefit human activities.

(5) Migration to other planets

For Mars, Jupiter, Saturn, Uranus, Neptune, their parameters (β, etc.) are collected in Ref. [6]. Regardless their atmospheres, using the above beat period formula, the human biological clocks on these planets are calculated, their beat periods are: Mars 8.6 years; Jupiter 10.6 years; Saturn 7.3 years; Uranus 1.04 years; Neptune 0.96 years. No one will be happy with the shorter life on these planets; migration to Mars always stays in our illusion. In addition, the β parameter of the earth is calculated based on the lunar orbit. To maintain the human biological clock, we must protect the moon, call for stopping landing on the Moon.

```
<Clet2020 Script>// [9]
double ABeta[10]={ 2.961520e+10, 1.377075e+14 , 2.581555e+15, 4.016793e+13,
7.183397e+13, 1.985382e+15, 2.077868e+15, 1.377075e+14,};
double Ar[10]={1, 1,   0.5326, 11.209, 9.449, 4.007, 3.882, 0.273,};
double AD[10]={1, 24, 24.6,   9.9,    10.35,   17.25, 16.1,655.68,};
int i,j; double beta,H,M,r,rs,rot,v1,v2, Year,T,Lamda,a,b,d;
int main(){j=50; rs=6.378e6; Year=24*3600*365.2422;
for(i=1;i<=7;i+=1) {
beta=ABeta[i]; H=SPEEDC*SPEEDC*SPEEDC/beta; r=Ar[i]*rs; d=AD[i];
rot=2*PI/(d*3600); v1=rot*r; v2=v1+1; a=v2*v2-v1*v1; T=4*PI*H/a;
T/=Year; Lamda=2*PI*H/(v2-v1); b=Lamda/(2*PI*r);
TextAt(100,j,"i=%d, v1=%f, v2=%f, T=%f, L=%e, b=%e",i,v1,v2,T,Lamda,b);
j+=30;}
}#v07=?>A
```

11. Conclusions

Relativistic matter wave provides a biological clock for human beings, it also governs planetary size and temperature. In this paper, the sunspot period, earth's atmosphere circulation with season clock and human biological clock are investigated, the clock formula is derived. As the results, the period of sunspot cycle is calculated to be 10.93 years, the human mean lifespan on the Earth is calculated to be 84 years, while the human mean lifespan reduces to 8.6 years on the Mars. A guidance of anti-ageing is proposed for the biological clock. The solar radius is determined as 7e+8 (m) with a relative error of 0.72%; the earth's radius is determined as 6.4328e+6 (m) with a relative error of 0.86%. The temperatures in the solar interior and in the earth's interior are also calculated by their relativistic matter waves. This approach gives a temperature 6031K in the solar convective layer, the solar core shell is estimated at a temperature 852K. The atmospheric temperature at sea level in the equatorial region is estimated to be 293K, and the mantle temperature is estimated to be 1467K.

References

[1] de Broglie, L. (1923) Waves and Quanta. Nature, 112, 540. https://doi.org/10.1038/112540a0

[2] de Broglie, L. (1925) Recherches sur la théorie des Quanta, Translated in 2004 by A. F. Kracklauer as De Broglie, Louis, on the Theory of Quanta. https://doi.org/10.1051/anphys/192510030022

[3] Marletto, C. and Vedral, V. (2017) Gravitationally Induced Entanglement between Two Massive Particles Is Sufficient Evidence of Quantum Effects in Gravity. Physical Review Letters, 119, Article ID: 240402. https://doi.org/10.1103/PhysRevLett.119.240402

[4] Guerreiro, T. (2020) Quantum Effects in Gravity Waves. Classical and Quantum Gravity, 37, Article ID: 155001. https://doi.org/10.1088/1361-6382/ab9d5d

[5] Carlip, S., Chiou, D., Ni, W. and Woodard, R. (2015) Quantum Gravity: A Brief History of Ideas and Some Prospects, International Journal of Modern Physics D, 24, Article ID: 1530028.

https://doi.org/10.1142/S0218271815300281
[6] Cui, H.Y. (2021) Relativistic Matter Wave and Quantum Computer. Kindle eBook, Amazon, Seattle.
[7] NASA. https://solarscience.msfc.nasa.gov/interior.shtml
[8] Schneider, S.E. and Arny, T.T. (2018) Pathways to Astronomy. 5th Edition, McGraw-Hill Education, London.
[9] Clet Lab (2022) Clet: C Compiler. https://drive.google.com/file/d/1OjKqANcgZ-9V56rgcoMtOu9w4rP49sgN/view?usp=sharing
[10] Orbital Debris Program Office, (2018) History of On-Orbit Satellite Fragmentations. 15th Edition, National Aeronautics and Space Administration, Washington DC.
[11] Wright, D. (2007) Space Debris. Physics Today, 10, 35-40. https://doi.org/10.1063/1.2800252
[12] Tang, Z.-M., Ding, Z.-H., Dai, L.-D., Wu, J. and Xu, Z.-W. (2017) The Statistics Analysis of Space Debris in Beam Parking Model in 78˚ North Latitude Regions. Space Debris Research, 17, 1-7.
[13] Cox, N. (2001) Allen's Astrophysical Quantities. 4th Edition, Springer-Verlag, Berlin. https://doi.org/10.1007/978-1-4612-1186-0
[14] Li,L.P. et al, (2021) Introduction to Atmospheric Circulation, 2nd edition, Science Press, Beijing.
[15] Cui,H.Y. (2022) Study of European Cold Streams Per 2.24 Years Based on Quantum Gravity Theory with Ultimate Acceleration,viXra:2211.0051,2022. https://vixra.org/abs/2211.0051
[16] wikipedia, https://en.wikipedia.org/wiki/List_of_longest-living_organisms#Animals
[17] Shanghai Municipal People's Government website, (2022-10-09) Shanghai Health Aging Action Plan was issued, https://www.shanghai.gov.cn/nw4411/20221009/e6a23fd0549d45d3a5d73f4fec5d4753.html
[18] Qinghai jgdj, (2022-02-22) The healthy Qinghai action in 2021 has been steadily promoted, https://www.qhjgdj.gov.cn/contentChild.jsp?contentId=14238
[19] Yunnan Provincial People's Government website, (2022-09-09) "The Decade of Yunnan" series press conference, https://www.yn.gov.cn/ynxwfbt/html/twzb/959.html
[20] China government website, (2022-11-30) National organization of centralized procurement of coronary stents, http://www.gov.cn/xinwen/2022-11/30/content_5729549.htm
[21] Cui,H.Y. (2022) Study of Earthquakes in Japanese Islands Using Quantum Gravity Theory with Ultimate Acceleration, viXra:2209.0149, 2022. https://vixra.org/abs/2209.0149
[22] Cui,H.Y. (2023) Determination of Solar Radius and Earth's Radius by Relativistic Matter Wave, Journal of Applied Mathematics and Physics, 11, 1, DOI: 10.4236/jamp.2023.111006